Atmospheric Research 176–177 (2016) 240–253

Contents lists available at ScienceDirect

Atmospheric Research

journal homepage: www.elsevier.com/locate/atmosres

Seasonal and interannual variation of radiation and energy fluxes over a rain-fed cropland in the semi-arid area of Loess Plateau, northwestern China

Xing Chen [a,b,c], Ye Yu [a,b,*], Jinbei Chen [a,b], Tangtang Zhang [a,b], Zhenchao Li [a,b]

[a] Key Laboratory of Land Surface Process & Climate Change in Cold & Arid Regions, Cold and Arid Regions Environmental and Engineering Research Institute, Chinese Academy of Sciences, Lanzhou 730000, Gansu, PR China
[b] Pingliang Land Surface Process & Severe Weather Research Station, Chinese Academy of Sciences, Pingliang 744015, Gansu, PR China
[c] University of Chinese Academy of Sciences, Beijing 100049, PR China

ARTICLE INFO

Article history:
Received 10 January 2015
Received in revised form 4 December 2015
Accepted 4 March 2016
Available online 11 March 2016

Keywords:
Radiation
Sensible heat flux
Latent heat flux
Soil moisture
Energy balance
Loess Plateau

ABSTRACT

Understanding the land–atmosphere interactions over the semi-arid area of Loess Plateau is important due to its special climate and unique underlying surface. In this study, two years' micrometeorological and energy flux observations from the Pingliang Land Surface Process & Severe Weather Research Station, CAS were used to investigate the seasonal and interannual variations of radiation budget and energy fluxes over a rain-fed cropland in the semi-arid area of Loess Plateau, with an emphasis on the influence of rain, soil moisture and agricultural production activities (such as crop type and harvest time) on the energy partitioning as well as the surface energy balance. The results revealed large annual variations in the seasonal distribution of precipitation, which gave rise to significant seasonal and interannual variations in soil moisture. Soil moisture was the main factor affecting radiation budget and energy partitioning. There was a negatively linear relationship between the albedo and the soil moisture. The main consumer of available energy varied among months and years with an apparent water stress threshold value of ca. 0.12 $m^3\ m^{-3}$, and the evapotranspiration was suppressed especially during the growing season. On an annual scale, the largest consumer of midday net radiation was sensible heat flux in 2010–2011, while it was latent heat flux in 2011–2012, which accounted for about 35% and 40% of the net radiation, respectively. The agricultural activity altered the sensitivity and variability of albedo to soil moisture, as well as energy partitioning patterns. The surface energy budget closures during Dec. 2010–Nov. 2011 and Dec. 2011–Nov. 2012 were 77.6% and 73.3%, respectively, after considering the soil heat storage. The closure was comparable to other sites in ChinaFLUX (49% to 81% of 8 sites). The patterns of energy partitioning and the water stress threshold found in the semi-arid cropland could be used to evaluate and improve land surface models.

1. Introduction

Land surface processes, which control the exchange of energy and mass fluxes between the surface and the atmosphere, is one of the most active research areas in climate change research (Wang et al., 2010). In recent years, global climate change research has promoted researches on surface radiation balance and energy balance in different regions around the world (Zhang et al., 2011a). The distribution and redistribution of solar energy modulate various meteorological environments (Baldocchi et al., 1997; Betts et al., 1996) and drive the Earth's climate system on local, regional, and ultimately global scales (Eugster et al., 2000). The partitioning of net radiation at the land surface into sensible and latent heat fluxes is one of the most important aspects of the land–atmosphere coupling (Gu et al., 2006), which determines the water vapor and heat content in the atmosphere and is critical in hydrological cycle, boundary layer development, and the regional or even global climate (Wilson and Baldocchi, 2000). Climate model results are especially sensitive to the seasonal and diurnal variations in surface energy partitioning (Bi et al., 2007; Dickinson et al., 1991) which is controlled by long-term interactions between biogeochemical cycling, climate and short-term interactions between plant physiology and the development of the atmospheric boundary layer (Wilson et al., 2002). In order to evaluate the long-term changes in energy balance and evapotranspiration, a number of field experiments have been carried out over various terrestrial surfaces throughout the world during the past decades (Gao et al., 2009). The eddy covariance technique (EC), the only method measuring turbulent fluxes over an ecosystem in a quasi-continuous long-term manner with minimal disturbance to the ecosystem, has become a standard tool for monitoring carbon, water and energy exchanges in ecosystems (Baldocchi, 2008; Baldocchi and Meyers, 1998). Within FLUXNET, in order to meet the emerging need for long-term studies of the biosphere-atmosphere exchange, a large

* Corresponding author at: Key Laboratory of Land Surface Process & Climate Change in Cold & Arid Regions, Cold and Arid Regions Environmental & Engineering Research Institute, Chinese Academy of Sciences, Lanzhou 730000, Gansu, PR China. Tel.: +86 931 4967168; fax: +86 931 4967168.
E-mail address: yyu@lzb.ac.cn (Y. Yu).

http://dx.doi.org/10.1016/j.atmosres.2016.03.003
0169-8095/

number of studies have been conducted to characterize the temporal and spatial variations in canopy-scale carbon dioxide, water vapor, and energy fluxes across diverse ecosystems (Baldocchi, 2008; Baldocchi et al., 2001; Bruemmer et al., 2008; Chen et al., 2012; Gu et al., 2015; Holwerda et al., 2013; Li et al., 2005; Liu et al., 2004; Liu and Feng, 2012; Liu et al., 2008a; Ma et al., 2003; Ryu et al., 2008; Su, 2002; Su et al., 2006; Suyker and Verma, 2008; Wu et al., 2007; Yao et al., 2011; Yu et al., 2006). It was observed that the energy balance at the surface was not always closed (Foken, 2008a; Foken, 2008b), and this problem could cause large differences between observations and model simulations and systematic errors (Cuxart et al., 2015).

In recent years, some field experiments have been conducted over the Loess Plateau in northwestern China (Chen et al., 2014; Guan et al., 2009; Huang et al., 2008; Li et al., 2012b; Wang et al., 2010, 2013; Wen et al., 2009, 2007; Yue et al., 2012; Zhang et al., 2009; Zhang et al., 2014; Zuo et al., 2009). Loess Plateau, located at the western boundary of the area affected by the East Asian summer monsoon and the South Asian summer monsoon (Zhang et al., 2011a), is the largest arid and semi-arid zone in China. Its surface characteristics have large spatial and seasonal variations and are sensitive to the change of East Asia summer Monsoon. The land surface processes over this region affect not only the regional climate and atmospheric circulations, but also the monsoon circulation in China (Wang et al., 2010). Global warming and human activities have affected the environment in the region very seriously and modified the temporal and spatial land surface physical processes to some extent (Zhang et al., 2011a). Although some scattered observations have been carried out in the Loess Plateau, many of the studies investigated only the short-term surface radiation and energy fluxes and mostly focused on one season or typical sunny days (Zhang et al., 2011a), little attention has been paid to long-term observations over the area (Li et al., 2012a; Wang et al., 2010; Zhang et al., 2013a, 2013b, 2011b), especially over cropland ecosystem. Land-use change is one of the most important aspects of global change, and farming is one of the major land-use change practices, which alters the species composition and function, removes substantial amounts of vegetation, modifies soil structure and affects the microclimate (Hammerle et al., 2006; Lei and Yang, 2010; Miao et al., 2009). Such land use changes have dramatic effect on the ecological and hydrological processes, including radiation balance, energy partitioning, aerodynamic characteristics, soil moisture and carbon cycle, which could in turn lead to potential significant changes in the regional and global climate (Baldocchi et al., 2001; Betts, 2001; Chen et al., 2009; Pielke et al., 1998), especially in the semi-arid area which is more sensitive to land use change (Liu et al., 2008b). An in depth understanding of the water vapor and energy exchange processes between the ground and the atmosphere and the related control factors in cropland ecosystem over the semi-arid area of Loess Plateau would benefit land surface model development and the evaluation of human effect on regional climate.

In this paper, comprehensive micrometeorological and energy flux data covering a 2-year period (December 2010–November 2012) collected at a typical rain-fed agricultural region of the Loess Plateau were used to: (1) analyze the variability of surface radiation, and characterize the seasonal and interannual variation of energy partitioning, (2) elucidate its relationship with land surface status as well as land use change caused by agricultural activities, and (3) evaluation the surface energy balance closure.

2. Materials and methods

2.1. Study site

The data used in this study were collected at the Pingliang Land Surface Process & Severe Weather Research Station, CAS (106°41′E, 35°34′ N, altitude 1630 m) located at a typical rain-fed agricultural region of the Loess Plateau in China (Fig. 1a), where the average annual precipitation is 500 mm with more than 70% concentrated in the East Asian monsoon season from June to September. The total annual precipitation varies significantly from year to year putting the region in alternating drought and flood conditions. The soil at the site is dominated by silty loam with a high proportion of silt (clay: 9.8%, silt: 76.6% and sand: 13.6%) and the agricultural economy is dominated by winter wheat and maize with some millet, soybean and benne. The measurement site is on the mesa of the Loess Plateau, with relatively flat surroundings. More details about the site can be found in Wen et al. (2009) and Zhang et al. (2014). The main crops were winter wheat with some maize during 2011 as showed in Fig. 2a, while they were dominated by winter wheat with some soybean and maize during 2012 (Fig. 2b). The seeding and harvest time of the crops are listed in Table 1.

2.2. Measurement and data processing

Surface radiation was measured with a net radiometer (CNR-1, Kipp & Zonen Inc., Netherland) at 1.5 m above the ground, which consisted of four radiometers to measure the incoming and reflected short-wave radiations, and the incoming and outgoing long-wave radiations. Soil temperature and water content were measured with thermistors (107, Campbell Scientific Inc., USA) and TDR sensors (CS616, Campbell Scientific Inc., USA) respectively at four depths (5, 10, 20 and 40 cm). Soil heat fluxes were measured with heat flux plates (HFP01, Hukseflux Inc., Netherland) at two depths (5 and 20 cm). Surface soil heat flux was corrected for storage above the heat flux plate at 5 cm depth, the data from the 20 cm plate was not used in this paper. Air temperature and humidity were measured with temperature and relative humidity probes (HMP45C, Vaisala Inc., Finland) at 2 m height. Wind speed and wind direction were measured using propeller anemometers (034B, Met One Inc., USA) at 2 m height and precipitation was measured with a tipping bucket rain gauge (52202, R M Young Inc., USA). The EC system, including an open-path infrared gas analyzer (LI-7500, Li-Cor Inc., USA) and a fast response three-dimensional sonic anemometer (CSAT3, Campbell Scientific Inc., USA), was used to measure the exchange of energy and water vapor in the ecosystem at 2.95 m above the ground. Basic meteorological parameters were measured at 10-min intervals, while the EC system sampled at 10 Hz. All the basic meteorological measurements were conducted at a distance of about 15 m to the east-southeast of the EC system, and the surface crop type was the same as that under the EC system.

Sensible and latent heat fluxes were calculated at an averaging time of 30 min in post-processing from the 10 Hz time series raw data. All of the necessary procedures for corrections and quality control of the turbulent flux calculation were applied during the post-processing. This included the statistical spike detection, planar fit coordinate transformation, sonic temperature correction, frequency response correction and Webb, Pearman, and Leuning correction of density fluctuations (WPL correction). And the quality control was made according to the number of missing values, stationary tests on covariance, integral turbulence characteristics test, residual w after planar fit and interdependency of flags due to corrections or conversions (Mauder et al., 2013). We also estimated the stochastic error and systematic error following Mauder et al. (2013). Periods with clearly bad half-hourly data likely caused by precipitation, malfunctions, or low quality were removed (using the flag system following Mauder et al.). The data gaps were not filled. There are about 25.2% (34.2%) missing or bad data for sensible (latent) heat fluxes during the period of December 2010-November 2011, and about 40.1% (47.5%) missing or bad data for the period of December 2011-November 2012, mainly caused by instrument malfunction and power supply problems during 19 January–8 April, 2012.

2.3. Footprint modeling

Most of the FLUXNET sites are operated in more or less homogeneous environments, however, small-scale within-site heterogeneity

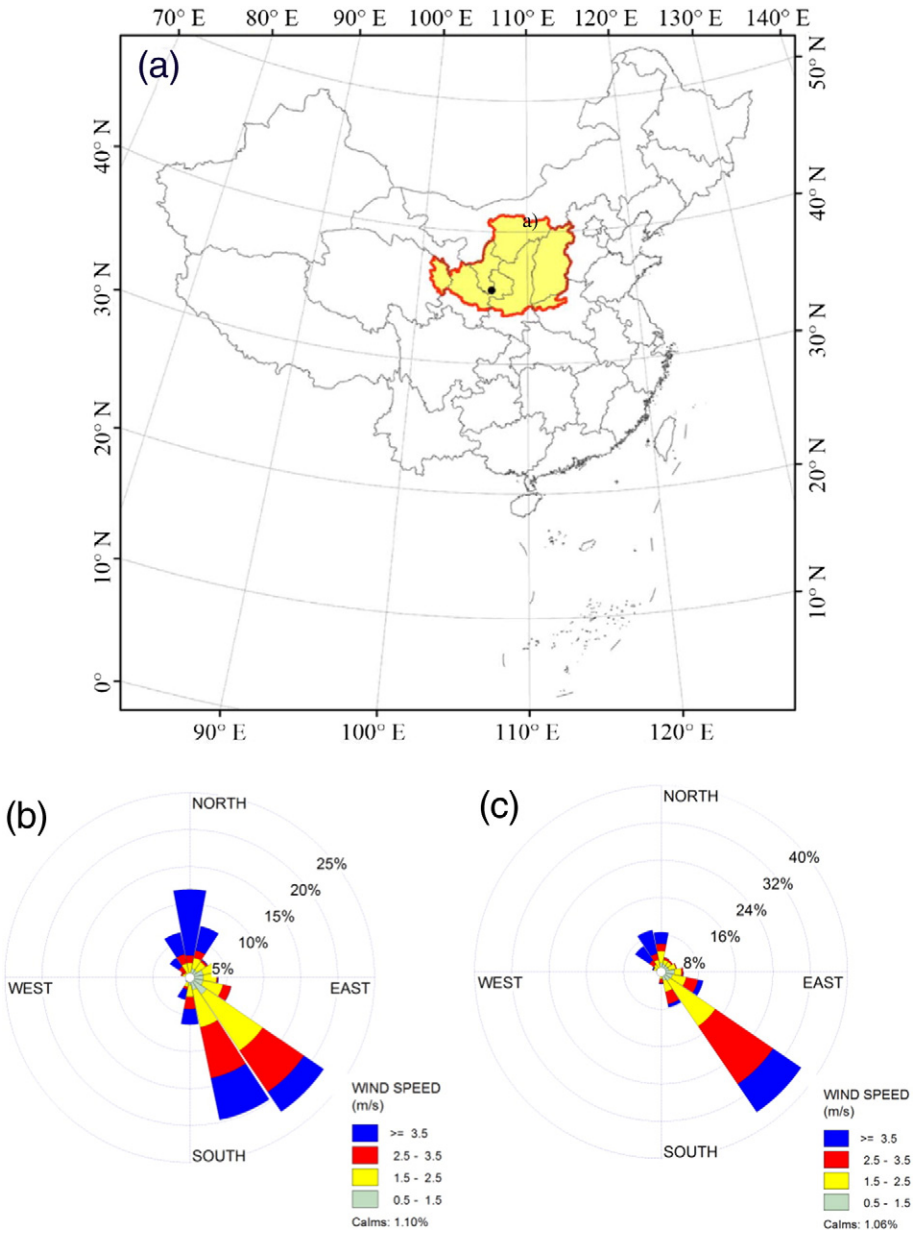

Fig. 1. (a) The Loess Plateau in China (red line showed the boundary of Loess Plateau) with the location of the observation site marked as dot, and the midday wind rose of the study site during (b) 2010–2011, (c) 2011–2012.

causes problems in ecosystem-scale eddy covariance measurements and they are considered a source of measurement uncertainty (Barcza et al., 2009; Gockede et al., 2004). In our study site, winter wheat, maize and soybean are main crops. Due to the climate, the growing season of the main crops have some overlap period over the Loess Plateau, which is special and different from the North China Plain (Lei and Yang, 2010). Therefore, we need to attribute the measured land–atmosphere exchange signal to specific crop cover for interpretation of the measured data. The problem was addressed by using a state-of-the-art footprint model and the information on crop cover in our site. A Lagrangian stochastic footprint model (Barcza et al., 2009; Kljun et al., 2004; Peters et al., 2011) was used to estimate the crosswind integrated footprint and the maximum source weight location of each half-hourly measurements. The applicability of the model is restricted to the following conditions: $-200 \le Z_m/L \le 1$; $u_* \ge 0.2$ m s^{-1}; $Z_m > 1$ m; $Z_m < h$ (Z_m is the measurement height, L is the Obukhov length, u_* is the friction velocity and h is the height of the planetary boundary layer). As our focus is on the energy partitioning during midday in the following section, we applied the model for midday measurements in the two years.

The footprint climatology of the EC measurement for the two years is shown in Fig. 2. It can be seen that there are two regions that contribute frequently to the measured signal: one is located at a distance of about 20–60 m to the southeast/south-southeast from the EC system, the second is located at the opposite side, i.e. to the north/north-northwest. The footprint climatology for the two years is similar, and they are the consequence of the prevailing wind directions (Fig. 1b and c) at the study site. Combining the crop cover map, we estimated the relative frequency of the contribution from different crop cover types to the measured signal (Table 1). Overall, during 2010–2011, the majority of the measured signal originates from winter wheat land, however, during 2011–2012, about 32.8% of the measured signal originates from soybean land (which was winter wheat land in previous year).

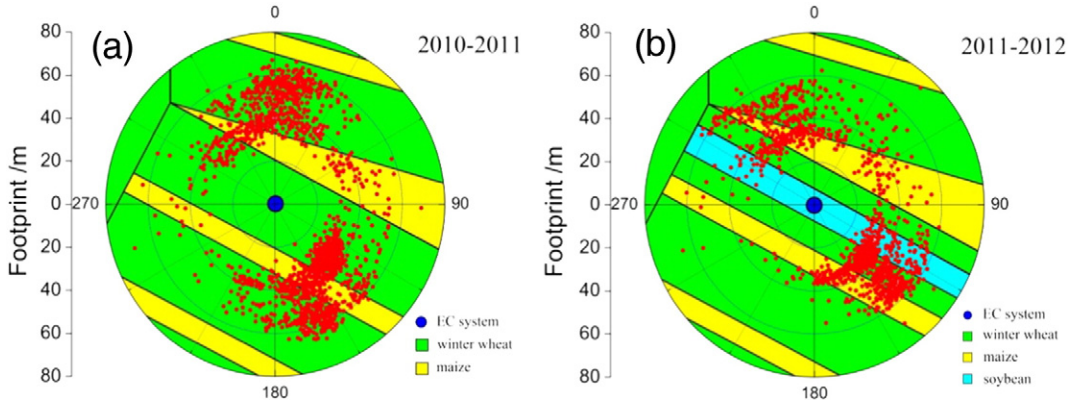

Fig. 2. Footprint climatology of the EC measurement during midday for (a) Dec. 2010 to Nov. 2011, and (b) Dec. 2011 to Nov. 2012. The maximum source strength locations are plotted as red dots. The crop cover map is also shown.

3. Results and discussion

3.1. Meteorological condition

Air temperature (T_a), water vapor pressure (e), soil volumetric water content (VWC) and precipitation (P) from December 2010 to November 2012 is presented in Fig. 3. The annual mean air temperature in 2010–2011 (2011–2012) was 7.8 (7.7) °C, which was close to the 38-yr-average annual mean air temperature (7.7 °C, which was calculated using the data from the nearest meteorological station located in Pingliang) in the study area. The water content in the upper soil (5 cm) was significantly lower than that in the deeper soil (10 and 20 cm) and responded readily to precipitation (Fig. 3c). Soil volumetric water content had large seasonal variations. It was strongly affected by precipitation and fluctuated with rainfall amount obviously. The maximum soil VWC at 5 cm was 0.297 $m^3\ m^{-3}$, which was about 57.7% of the soil porosity (0.52 $m^3\ m^{-3}$ for the silt loam in the study site). The seasonal and interannual variation of precipitation (P) was large (Fig. 3d) in the study area. The total precipitation was 615.6 and 453.1 mm in 2011 and 2012, respectively. Compared to the 38-yr-average annual P (486.7 mm), it was wet (slightly dry) in 2011 (2012). In 2011, P was unevenly distributed throughout the year, with 70% of the annual precipitation falling between July and September, while P distributed relatively even in 2012 and both the monthly precipitation and the number of days with more than 5 mm daily precipitation were more than that in 2011 during the growing season (March to June) of winter wheat (Fig. 3d and e).

3.2. Radiation components

Solar radiation is the energy source of the earth and drives energy exchange between the surface and the atmosphere. Seasonal variation of the solar radiation received by land surface depends mainly on the solar altitude and is significantly influenced by weather conditions and clouds. The daily mean downward shortwave radiation (DSR) fluctuated with weather conditions and reached the maximum of 360.2 W m^{-2} in the middle of June (Fig. 4), which is comparable to that observed in middle Gansu region (Wang et al., 2010). The daily mean upward shortwave radiation (USR) maximized in winter due to the high snow surface albedo. In addition, the USR was high with the increase of DSR in late spring and fell to relatively low values with the decrease of surface albedo due to the greening of vegetation and the increase of precipitation. Longwave radiation was less affected by weather conditions and reached the maximum in summer. The maximum daily mean downward longwave radiation (DLR) was 408.7 W m^{-2}, which was slightly larger than that observed over grassland in middle Gansu (Wang et al., 2010), while the maximum daily mean upward longwave radiation (ULR) was 459.2 W m^{-2}, which was slightly lower than that observed over grassland in middle Gansu (Wang et al., 2010). The upward longwave radiation was related to surface temperature ($R^2 = 0.99$), thus it had the same waveform with the surface temperature (not shown). While the downward longwave radiation was influenced by air temperature ($R^2 = 0.71$) and water vapor pressure ($R^2 = 0.83$).

Surface albedo characterizes the ability of surface to reflect the incoming solar radiation and is related to the conditions of underlying surface. Fig. 5 shows the variation of midday (11:00–15:00) mean surface albedo during the study period. The maximum midday mean surface albedo was 0.83, occurred after snow. With the melting of snow and infiltrating of water into the soil, the albedo decreased quickly in spring. During the growing season, the albedo decreased slightly with the growth of crop. The surface was bare and sparsely vegetated after the harvest of winter wheat at the end of June in 2011, after which the surface albedo was relatively low and lower than that before the harvest as wet soil is dimmer than vegetation. There were periods when surface albedo increased day by day when soil was gradually drying out until the next rainfall. This cycle was obvious between July and September 2011. Soil moisture is a key parameter controlling surface albedo (Wang et al., 2010). A decrease of surface albedo with increasing soil moisture was found over the grassland in middle Gansu over Loess Plateau (Guan et al., 2009; Li et al., 2012a), the bare landscape over the north region of Mt. Everest (Chen et al., 2012), and the cropland and grassland in the semiarid area of northeastern China (Liu et al., 2008a). An inverse correlation between the albedo and the soil moisture was also found in our study site, especially after the harvest, as shown in Fig. 6 & Table 2. The albedo was less sensitive to soil moisture during the growing season compared with that after the harvest.

The albedo during the growing season in our study area was lower than the cropland in middle Gansu over the Loess Plateau (Zhang et al., 2011a), which was related to more precipitation, and thus wetter soil and better crop growth in our site. The maximum albedo observed in winter was higher than that of cropland in middle Gansu (Zhang et al., 2011a), probably due to the heavy snow in our study period.

Table 1
Cropping information and relative importance of the crop cover types to the measured signal for Dec. 2010 to Nov. 2012.

Crop cover	Seeding time	Harvest time	2010–2011	2011–2012
Winter wheat	September	Late June	72.6%	33.0%
Maize	March	September	27.4%	34.2%
Soybean	April	September	–	32.8%

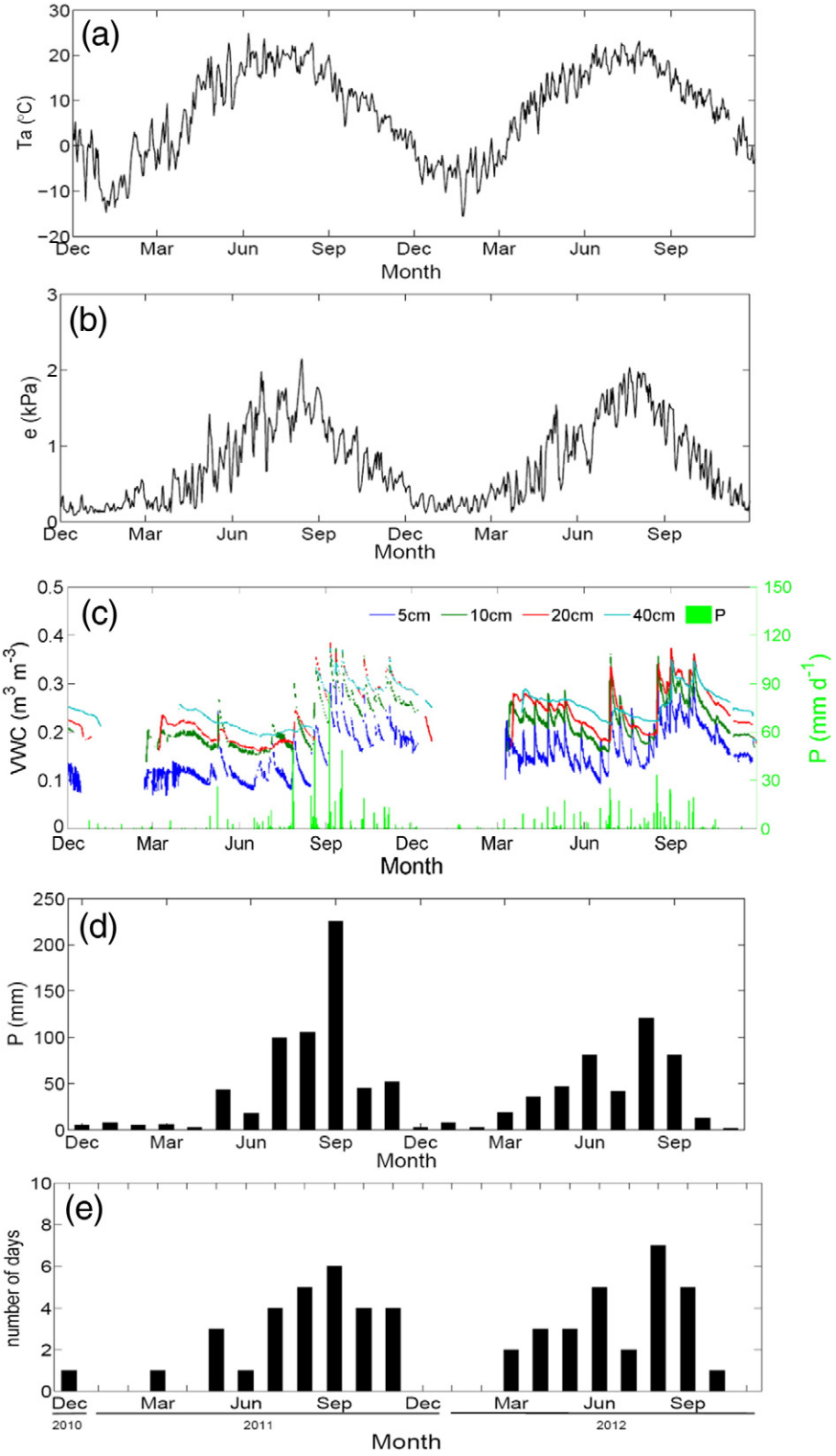

Fig. 3. (a) Daily mean air temperature (T_a), (b) daily mean water vapor pressure (e), (c) soil volumetric water content (VWC) and daily precipitation (P), (d) monthly precipitation (P), and (e) number of days with daily precipitation larger than 5mm, from Dec. 2010 to Nov. 2012.

Due to the large interannual variations in precipitation and agricultural activity, there were considerable differences in surface radiation budget among years. The annual mean albedo in 2011–2012 was smaller than that in 2010–2011 as listed in Table 3, resulted in less shortwave radiation reflected into the atmosphere. The surface temperature and soil temperature were slightly lower in 2011–2012, resulted in less upward longwave radiation. All these contributed to the more net radiation in 2011–2012.

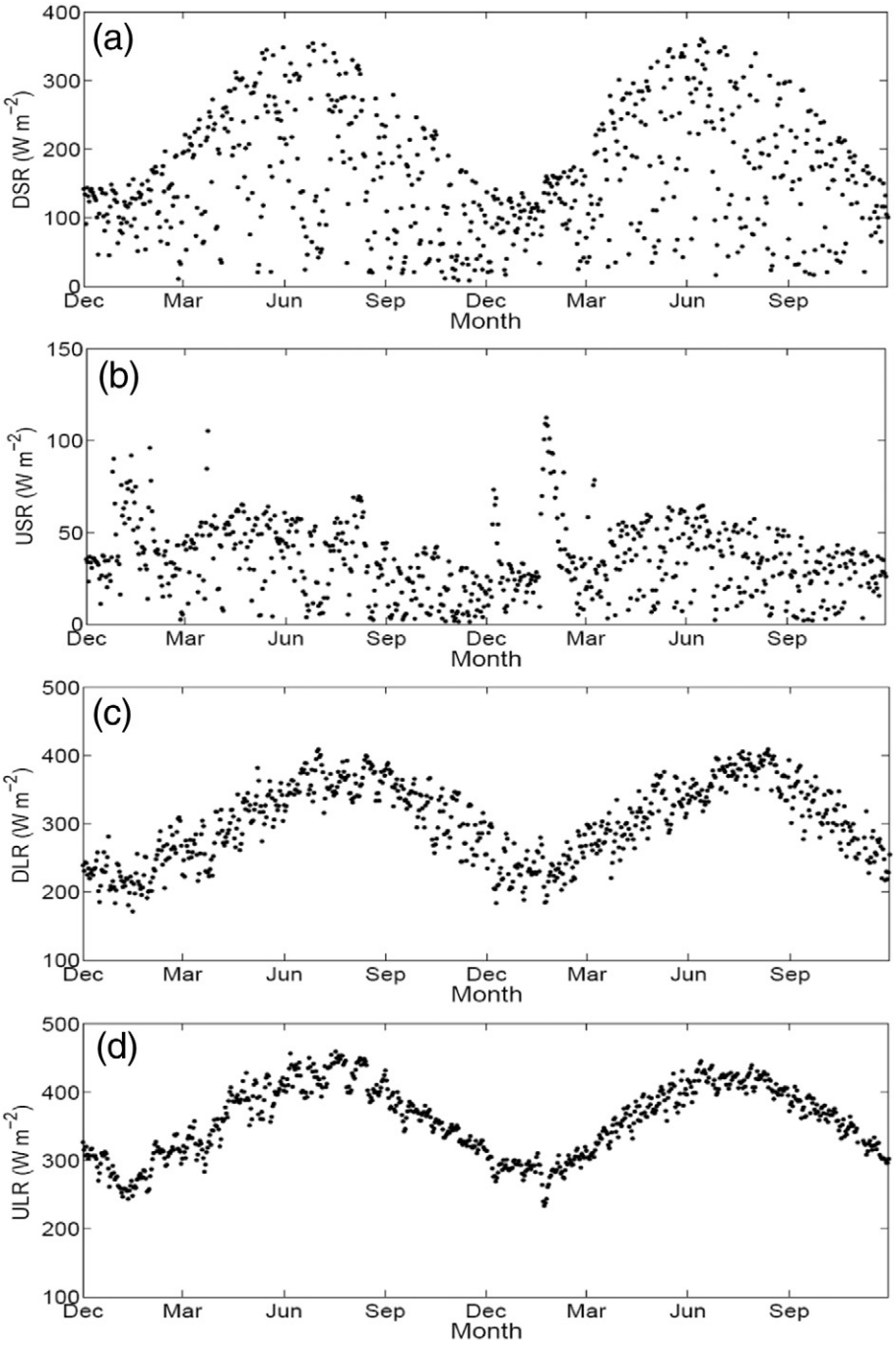

Fig. 4. Daily mean (a) downward shortwave radiation (DSR), (b) upward shortwave radiation (USR), (c) downward longwave radiation (DLR), (d) upward longwave radiation (ULR) from Dec. 2010 to Nov. 2012.

3.3. Surface energy fluxes

3.3.1. Diurnal, seasonal and interannual variations

The radiation received by surface drives the energy exchange between the surface and the atmosphere. As shown in Fig. 7a, the diurnal cycle of monthly mean net radiation (R_n) reached the daily peak during 12:00–13:00 Beijing time, while the daily peak of H_s (LE) lagged for about 0–1.5 (2.0) hours. The small positive value of LE (about 10 W m^{-2}) during nighttime indicates that there were evapotranspiration (ET) during night, while the small negative value of H_s (about −10 W m^{-2}) indicates that the surface obtained energy from the atmosphere due to its cooling by emitting radiation during night or supplying energy for ET. In general, G_0 was lower than H_s and LE, with higher values during spring and summer and lower values during autumn and winter. The slightly negative value of G_0 (about −20 W m^{-2}) during night indicates that energy was transported from soil to the surface.

The seasonal variation of energy exchange was shown in Fig. 7b, c and Table 4. The midday mean H_s, LE and G_0 ranged from 53.6 to 177.6 W m^{-2}, 37.4 to 235.8 W m^{-2}, and 4.3 to 108.4 W m^{-2}, respectively. The seasonal variations in LE and H_s during 2011–2012 (Fig. 7c) were similar to other ecosystems, which had been interpreted as responses to the emergence of new leaves in spring and the rapid senescence of leaves from early September (Chen et al., 2009; Wilson and Baldocchi, 2000; Wu et al., 2007). However, the seasonal patterns of the LE and H_s during 2010–2011 (Fig. 7b) was significantly different from that during 2011–2012. During 2010–2011, the midday H_s/R_n

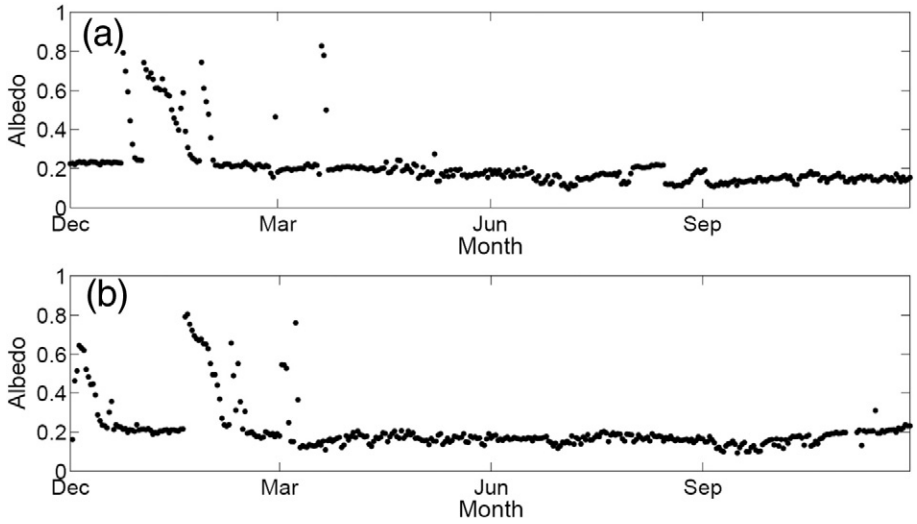

Fig. 5. Variation of midday mean surface albedo (a) from Dec. 2010 to Nov. 2011, (b) from Dec. 2011 to Nov. 2012.

ranged from 12.0% to 76.1%, while the midday LE/R_n ranged from 7.5% to 75.8%, and the largest consumer of net radiation shifted between *LE* and H_s. One of the reasons for the seasonal fluctuation in H_s and *LE* was the distribution of precipitation, for instance, during the growing season of 2011, *LE* was lower than H_s in April due to low precipitation (Table 4), while it became greater than H_s in May with the increase of precipitation, but fell slightly below H_s when the precipitation decreased in June, and *LE* was obviously higher than H_s in September 2011 when the maximum monthly precipitation of 2011 occurred (Fig. 3d, Table 4). Another reason was the agricultural activities, i.e. in July and August of 2011, *LE* was only slightly higher than H_s though the precipitation increased (Table 4), which was related to the lower or no active plant transpiration (soil was bare after the harvest of winter wheat). The harvest of winter wheat could lead to the decrease of *LE as* vegetated surface produces more *LE* than bare soil due to transpiration. While, during 2011–2012, more precipitation was available in spring and it was well-distributed in the whole growing season (Fig. 3d and e), in addition, there were soybeans in the footprint of surface energy fluxes after the harvest of winter wheat, all of these made the *LE* higher than H_s from April to September with the daily peak of *LE* more than doubled that of H_s and reached the maximum of 277.6 W m^{-2} in July 2012.

Compared with the cropland in middle Gansu (Zhang et al., 2011a), the *LE* in our studied ecosystem was larger and there were more months during which *LE* was larger than H_s. The seasonal variation of energy fluxes were also different from that in middle Gansu cropland where *LE* increased with R_n and reached the maximum in early summer which were larger than H_s for only few months, then fell as quickly as R_n.

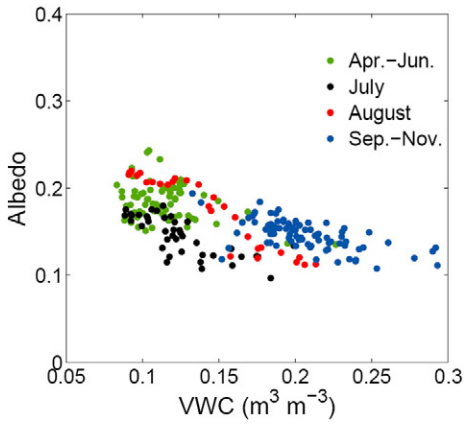

Fig. 6. Relationships between midday mean surface albedo and soil volumetric water content (*VWC*) from Apr. to Nov. 2011.

3.3.2. Bowen ratio

Fig. 8 shows the variation of the midday Bowen ratio which is defined as the ratio of H_s and *LE* and was generally used to investigate the effect of surface condition on energy partitioning. The variability in the Bowen ratio was large, ranged from 0.04 to 7.86, which was related to the variation of soil moisture and vegetation. As a result of the frozen soil and the degeneration of vegetation in winter, R_n was primarily consumed by H_s (Fig. 7, Table 4) and the Bowen ratio was large. With the increase of precipitation and the growth of crop, *LE* increased significantly (Fig. 7, Table 4) and the Bowen ratio fell quickly from spring. As the spring of 2011 was dry and the surface was bare in summer after the winter wheat harvest, the Bowen ratio was generally around or above 2 except after rainfall evens. While the spring and the summer of 2012 were relatively wet and there was some soybean after the harvest of winter wheat, the Bowen ratio was generally below 1. During the autumn of 2011, the Bowen ratio maintained below 1 due to high soil volumetric water content, while the Bowen ratio was below 1 in early autumn of 2012 and then increased to above 3 in late autumn when soil was drying out.

The Bowen ratio in our study site was comparable to the shrub savanna in West Africa (Bruemmer et al., 2008) during wet season, but was much lower than the shrub savanna during dry season. It was higher than the irrigated maize-based cropland (Suyker and Verma, 2008) during the growing season of 2011, while was slightly higher during the growing season of 2012. The annual midday Bowen ratio were 1.61 and 1.23 in 2011 and 2012, respectively, which were much lower than some cropland and steppe sites in Inner Mongolia (Chen et al., 2009). The mean Bowen ratio for winter wheat (averaged for April and May) were 1.14 and 0.53 in 2011 and 2012, respectively, that were much higher than an irrigated wheat site in the North China

Table 2
Statistical parameters of the relationships between midday mean surface albedo and soil VWC from Apr. to Nov. 2011.

Period	Surface	Slope	Intercept	R^2
Apr.-Jun.	Wheat	−0.31	0.22	0.11*
July	Ploughed	−0.62	0.22	0.55*
August	Bare	−0.99	0.32	0.90*
Sep.-Nov.	Sparsely vegetated	−0.36	0.22	0.42*

* Relationships are significant at the 99% confidence interval.

Table 3
Annual mean values of radiation components, albedo, surface temperature (Ts), 5-cm soil temperature (T_5) and soil heat flux (G_0). The radiation components and soil heat flux are in W m^{-2} and the temperatures are in °C.

Year	DSR[a]	USR[a]	DLR[a]	ULR[a]	R_n[a]	Albedo	Ts	T_5	G_0
2010–2011	159.9	34.9	302.4	359.1	68.3	0.218	7.8	12.1	4.0
2011–2012	163.7	34.6	303.6	355.8	76.9	0.211	7.7	11.2	0.3

[a] DSR: downward shortwave radiation, USR: upward shortwave radiation, DLR: downward longwave radiation, ULR: upward longwave radiation, R_n: net radiation.

Plain (Lei and Yang, 2010), indicating that the evapotranspiration was suppressed in our study site.

3.3.3. Energy partitioning

The partitioning of net radiation absorbed by the surface into H_s, LE and G_0 was affected by land surface conditions. On an annual scale, the largest consumer of midday net radiation was sensible heat flux in 2011, which accounted for about 35% of R_n, while it was the latent heat flux in 2012, which accounted for about 40% of R_n. The average midday LE/R_n were about 32% and 40% in 2011 and 2012, respectively, which were lower than some irrigated croplands of 59% and 60% (Lei and Yang, 2010; Suyker and Verma, 2008). During the rapid growing season of winter wheat (March to May), the average midday LE/R_n were about 34% and 46%, respectively, in 2011 and 2012, which were much lower than other croplands, such as, irrigated winter wheat agro-ecosystem of 83% (Lei and Yang, 2010), summer maize of 57% (Lei and Yang, 2010), and irrigated maize or soybean of about 70% (Suyker and Verma, 2008), indicating that it was water limited in our study site. Therefore, we investigated the effects of soil moisture on surface energy partitioning as shown in Fig. 9. Overall, H_s/R_n decreased with increasing soil moisture, while LE/R_n increased with soil moisture. This overall pattern resulted in the fluctuation of H_s and LE (Fig. 7b). As the precipitation was the only source of the soil moisture, the partitioning of the surface energy was sensitive to the changes in precipitation in the studied semi-arid agroecosystem, and the largest consumer of net radiation shifted between LE and H_s mainly depending on precipitation. There was an apparent water stress threshold value of ca. 0.12 m^3 m^{-3}, above that, LE/R_n exceed H_s/R_n. However, there were only 30% of days with the midday VWC greater than this threshold during May to June, 2011. The evapotranspiration of crops was suppressed in our study site, resulted in the much lower LE/R_n than other agro-ecosystem (Lei and Yang, 2010; Suyker and Verma, 2008). While during May to June, 2012, there were more than 70% of days with midday VWC greater than 0.12 m^3 m^{-3} and the LE/R_n was obviously higher than 2011

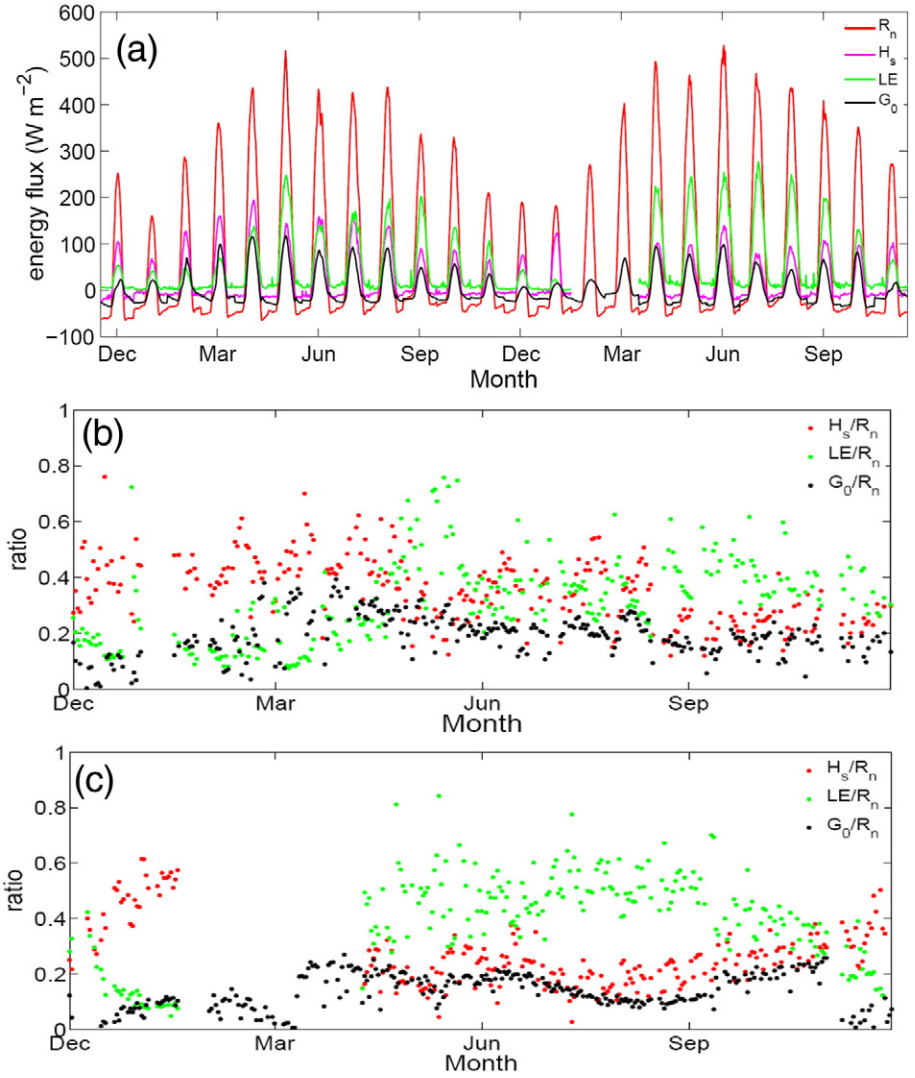

Fig. 7. (a) Diurnal cycle of the monthly mean net radiation (R_n), sensible heat flux (H_s), latent heat flux (LE) and surface soil heat flux (G_0), and ratios of midday sensible heat flux, latent heat flux and surface soil heat flux to net radiation (b) from Dec. 2010 to Nov. 2011, (c) from Dec. 2011 to Nov. 2012.

Table 4
Monthly summaries of total precipitation (*P*) in mm, and midday means of 5-cm soil water content (*VWC5*) in $m^3\ m^{-3}$, net radiation (R_n) in W m^{-2}, air temperature (*Ta*) in °C, vapor pressure deficit (*VPD*) in kPa, surface temperature (*Ts*) in °C, sensible heat flux (H_s) in W m^{-2}, latent heat flux (*LE*) in W m^{-2}, and surface soil heat flux (G_0) in W m^{-2}, from Dec. 2010 to Nov. 2012.

Year	Month	Surface[a]			*P*	*VWC5*	R_n	*Ta*	*VPD*	*Ts*	H_s	*LE*	G_0
		Wheat	Maize	Soybean									
2010	12	√		–	5.3	–	222.1	1.3	0.54	6.4	90.7	50.9	13.8
2011	1	√		–	7.7	–	141.6	−8.4	0.16	−4.1	57.2	37.4	18.5
	2	√		–	5.1	–	258.5	1.6	0.39	10.2	111.2	42.7	46.4
	3	√	√	–	6.0	0.112	336.2	3.7	0.60	14.2	147.8	62.0	81.2
	4	√	√	–	2.5	0.112	395.4	14.6	1.33	25.7	177.6	127.1	108.4
	5	√	√	–	43.6	0.130	441.7	17.2	1.27	23.0	123.9	216.2	103.3
	6	√	√	–	18.3	0.103	389.2	22.1	1.60	28.2	143.6	135.5	77.6
	7		√	–	99.6	0.127	389.4	22.8	1.42	34.5	140.8	152.3	79.1
	8		√	–	105.4	0.142	406.9	20.7	0.96	29.5	127.1	167.4	83.4
	9		√	–	224.8	0.218	304.7	14.2	0.50	18.3	77.1	177.3	44.1
	10	√			45.4	0.194	294.3	10.5	0.47	13.8	75.1	120.7	50.1
	11	√			51.9	0.203	189.1	4.5	0.22	7.0	53.6	83.1	28.5
	12	√			2.7	–	167.7	−2.3	0.23	−0.1	65.0	37.6	4.3
2012	1	√			8.0	–	163.4	−4.5	0.24	0.2	103.2	18.9	12.7
	2	√			2.4	–	243.2	−2.8	0.26	3.5	–	–	19.7
	3	√	√		19.0	0.147	360.5	4.8	0.50	10.5	–	–	56.8
	4	√	√	√	35.9	0.154	438.1	13.9	1.08	20.6	93.5	196.5	86.3
	5	√	√	√	46.8	0.160	416.8	17.1	0.98	23.7	88.6	218.3	67.2
	6	√	√	√	80.9	0.139	484.5	21.8	1.45	31.8	125.9	227.6	88.0
	7		√	√	42.0	0.166	430.1	22.7	1.17	27.5	69.3	235.8	54.2
	8		√	√	120.3	0.190	419.6	21.1	0.84	28.4	83.4	223.0	40.2
	9		√	√	81.0	0.246	363.6	15.2	0.65	20.1	98.1	186.6	54.8
	10	√			12.7	0.197	320.1	12.2	0.75	16.8	88.8	118.4	66.8
	11	√			1.4	0.145	256.5	3.8	0.52	9.1	93.0	63.5	7.2

[a] Surface crop types are shown in Fig. 2. √ means the crop was in the land, blank means the crop was harvested, – means no soybean during 2010 to 2011.

(Fig. 7c) though the total precipitation was less compared to 2011. This indicated that the distribution of precipitation was more important than the total precipitation amount. In addition, when the main crop (wheat) was harvested (Fig. 9b and c) or all the crops were harvested (Fig. 9d), the LE/R_n was lower than that before harvested (Fig. 9a) at the same soil moisture condition. This means that the agricultural activities could result in decreased latent heat fraction because of the shortened plant growing period (Chen et al., 2009), so the LE/R_n during July–August 2011 was much lower than that in 2012 due to the earlier harvest of the winter wheat in 2011 as compared to the harvest of soybean in 2012.

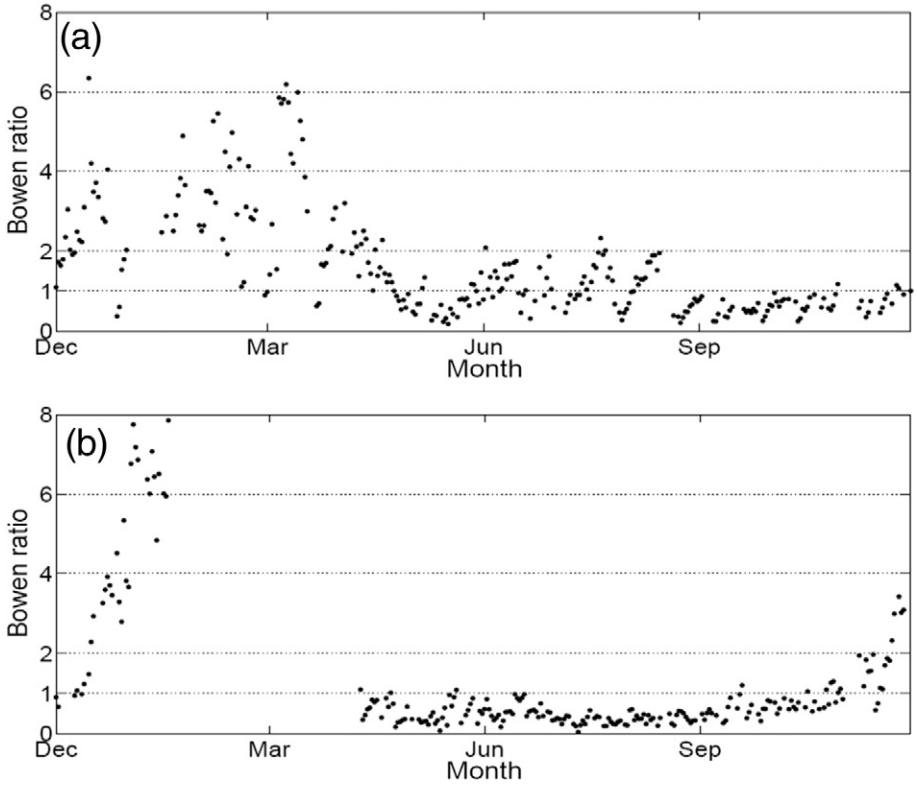

Fig. 8. Variation of midday Bowen ratios (a) from Dec. 2010 to Nov. 2011, (b) from Dec. 2011 to Nov. 2012.

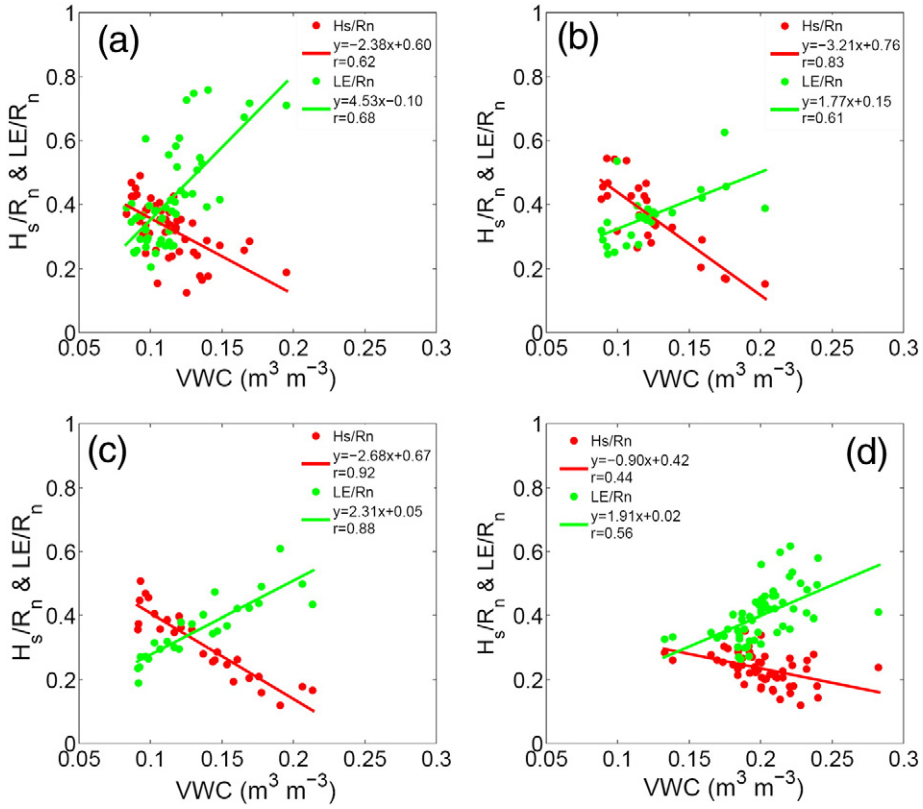

Fig. 9. Relationships between the ratios of midday H_s and LE to R_n with soil volumetric water content for (a) May to June, (b) July, (c) August, and (d) September to November, 2011.

3.4. Energy balance closure

The surface energy balance can be expressed as

$$Rn = Hs + LE + G_0 + Re \quad (1)$$

where R_e is the residual energy involving various processes, such as canopy heat storage, photosynthesis, respiration and advection. Surface soil heat flux G_0 is estimated as the sum of soil heat flux measured at 5cm depth and ground heat storage above the soil heat flux plate. Fig. 10 showed the intercomparison of $(H_s + LE)$ and $(R_n - G_0)$ for a full year. The energy balance closure, defined as the ratio of measured $(H_s + LE)$ and available energy $(R_n - G_0)$, was 77.6% and 73.3% for 2010–2011 and 2011–2012 using 30-min dataset, respectively, which falls within the closure (using linear regression slope for 30-min dataset) of 49% to 81% obtained by Li et al. (2005) for 8 sites in ChinaFLUX, and the use of daily averages could improve the energy closures in our site to 90.2% and 78.8%, respectively. Overall, the surface energy balance closure in our site was good compared with other sites in ChinaFLUX. There are various sources for the energy imbalance (Foken, 2008a; Leuning et al., 2012). Wen et al. (2009) argued that the degree of energy imbalance is considerable in the Loess Plateau mainly due to the heat storage in the soil, vegetation canopy and near surface air layer. Their estimated heat storage in millet canopy during summer in the study site was about −10 to 25 W m^{-2}. Meyers and Hollinger (2004) reported that the storage in maize and soybean land were generally a small fraction (<5%) of the net radiation. An analysis of the role of ground heat storage to the energy balance in the study site in our previous work (Chen et al., 2014) indicated that ground heat storage should not be neglected, which was also investigated by Li et al. (2012b). The energy balance closure considering the ground heat storage was still lower than that at grassland in middle Gansu (Li et al., 2012b; Wang et al., 2010). The signature of the measured fluxes coming from different source areas was one of the reasons for energy imbalance (Foken, 2008b). At our study site, the source areas of

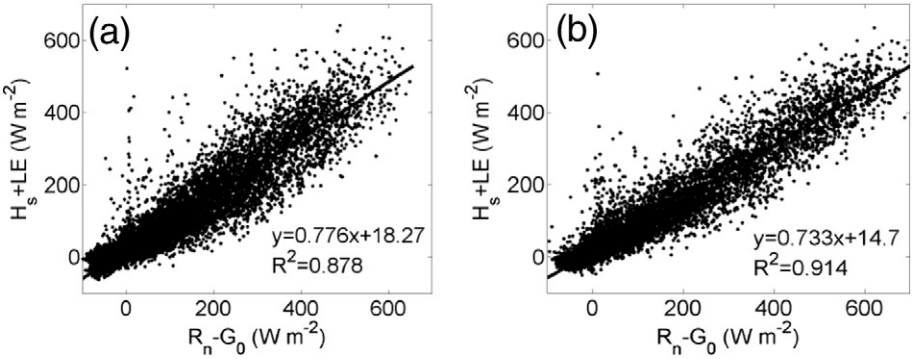

Fig. 10. Surface energy balance closure for (a) Dec. 2010–Nov. 2011, and (b) Dec. 2011–Nov. 2012.

Table 5
Average values of the terms of the surface energy balance[a] from Dec. 2010 to Nov. 2011.

		R_n	H_s	LE	G_0	Imb
1100–1500	Annual	314.5	114.8	116.9	61.3	39.3
	Winter	205.7	87.3	44.2	25.5	54.2
	Spring	391.1	151.7	139.0	97.5	8.8
	Summer	395.2	140.0	155.7	80.0	36.5
	Autumn	263.0	71.3	133.5	41.0	62.5
2300–0300	Annual	−40.7	−10.6	7.9	−21.4	−18.9
	Winter	−46.0	−13.3	5.2	−22.2	−20.9
	Spring	−48.0	−12.3	9.1	−22.3	−21.9
	Summer	−40.8	−10.4	8.4	−23.2	−15.3
	Autumn	−27.9	−5.2	8.5	−17.8	−16.8

[a] Units: W m^{-2}. The imbalance (*Imb*) is the average of individual imbalances.

turbulent fluxes contained different crops, whereas those of R_n and G_0 were from a single kind of cropland.

Cuxart et al. (2015) estimated the surface energy balance for a site in the eastern Ebro Basin, Catalonia, using the annual and seasonal averages for both noon and midnight. Here we also calculated the annual and seasonal averages of the surface energy balance for the midday (11:00–15:00) and midnight (23:00–03:00) (Table 5). The imbalance (*Imb*) at midday was large in autumn and winter, while it was small in spring. During midday, the values of the imbalance were approximately 2% of R_n in spring and 26% in winter, whereas for the midnight, the imbalance accounted for about 37% to 60% of R_n. Compared to other recent studies, such as in the Ebro Valley, Cuxart et al. (2015) reported imbalances of about 27% to 34% of R_n during the daytime and about 24% to 33% during nighttime, our imbalances were small in the midday, however the values at midnight were relatively large.

To investigate the reasons for energy imbalance, Cuxart et al. (2015) analyzed the relationship of the imbalance with the terms of surface energy balance for all hours in the Ebro Valley site and found the imbalance was linearly related to R_n. Here we also analyzed this relationship and the results are shown in Fig. 11. A linear relationship between the imbalance and R_n, either during night or daytime, was also found in our site similar to that documented in Cuxart et al. (2015) except the small magnitude of the imbalance at our site. It means that the radiative forcing is not compensated by the main terms of the SEB (Cuxart et al., 2015). However, the relationships of the imbalance with the H_s, LE, and G_0 were different from that in the Ebro Valley site, especially at high values of H_s, LE and G_0, when some deficits exist. We found that the large imbalance deficit ($Imb < -100$ W m^{-2}) mainly occurred during 13:00 to 16:00 (accounting for 70% of occasions with $Imb < -100$ W m^{-2}) in spring and summer. It happened mainly due to the short time cloudy which resulted in the decrease of incoming (R_n) (Table 6), whereas the expense of energy by H_s and LE stayed the same except the little decrease of G_0 (Table 6), which means that there was a time delay of the energy exchange at land surface from the radiative forcing as shown in the diurnal cycle in Section 3.3.1.

In addition, we investigated the relationship between the Imb/R_n and several air and soil variables during the midday (11:00–15:00), as very large imbalances was found to be related to high soil moisture especially in warm conditions in Cuxart et al. (2015) for the Ebro Valley site through a similar analysis. As shown in Fig. 12a, the energy imbalance showed a dependence on u_*, and the ratio of the imbalance decreased with the increasing u_*. Friction velocity, to some extent, reflects the development of turbulence and low u_* often indicates poorly developed turbulence (Wu et al., 2007). This explains the great energy imbalance in autumn and winter, as well as during midnight, when u_* was low. It seemed that the ratio of imbalance was high when the weather was cold (Fig. 12b, d, and e), or the soil was wet (Fig. 12f), pointing to the effect of the heat storage in frozen soil, vegetation canopy and near surface air layer. While, there was no clear relationship between the ratio of imbalance and the specific humidity (q, Fig. 12c).

Overall, the energy balance closure statistics at our site were reasonably comparable to other sites. The eddy covariance method is susceptible

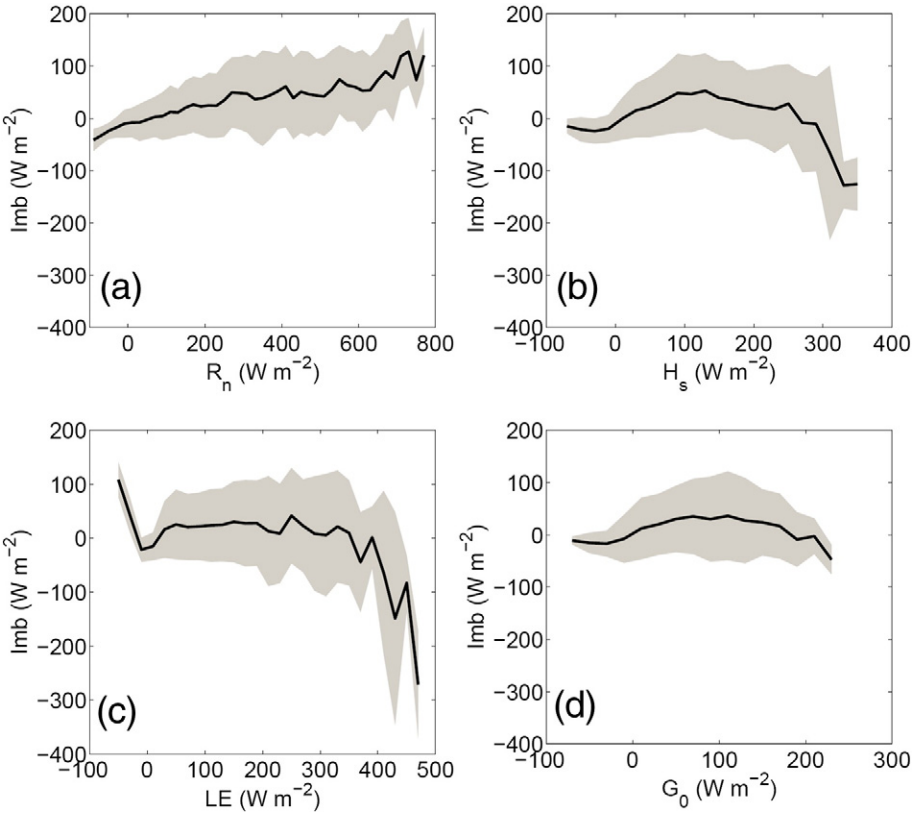

Fig. 11. The imbalance as a function of the terms of the surface energy balance (comparable to Fig. 4 in Cuxart et al., 2015). The black line represents the average values of the imbalance for a particular interval of the SEB term and the shaded grey area the standard deviation.

Table 6
Average values of the terms of the surface energy balance[a] for the periods with imbalance deficit and different hours before the occurrence of the imbalance deficit.

	R_n	H_s	LE	G_0	Imb
Time−2h	499.3	167.8	198.3	118.9	23.0
Time−1.5h	497.4	173.9	197.6	120.8	14.0
Time−1h	483.7	172.4	197.1	118.7	0.4
Time−0.5h	456.5	168.4	195.0	112.4	−18.1
Imb<−100	329.0	167.9	222.1	96.4	−157.3

[a] Units: W m^{-2}. The imbalance is the average of individual imbalances.

to errors when the surface energy balance does not close, however, its strengths in measuring interannual variability of surface energy fluxes are apparent because bias errors tend to be constant from year to year (Ryu et al., 2008).

4. Conclusions

In this study, we reported the seasonal and interannual variability of the radiation, the energy fluxes and the energy balance closure over a rain-fed cropland in the semi-arid area of Loess Plateau, Northwest China, based on 2-year's flux measurements spanning from December 2010 to November 2012.

The studied agro-ecosystem located in a semi-arid area, where the precipitation has large seasonal and interannual variations. Soil volumetric water content was far from saturation and the evapotranspiration was suppressed due to the water stress in this semi-arid cropland, especially during the growing season. An apparent water stress threshold value of ca. 0.12 m^3 m^{-3} was found for the studied crop site. In this semi-arid area, soil moisture (distribute of precipitation) was the main factor affecting the radiation budget and surface energy partitioning. Soil moisture altered the main consumer of available energy, which could determine the development of boundary layer and the regional climate. As climate models are sensitive to surface energy partitioning, the pattern of the energy partitioning in our site could be used to evaluate the models.

Agricultural activity affects the function of soil moisture by altering the sensitivity and variability of albedo to soil moisture, as well as energy partitioning patterns. This short-term change in land use caused by agriculture activities should be considered in models. And the energy portioning over different crop species need to be

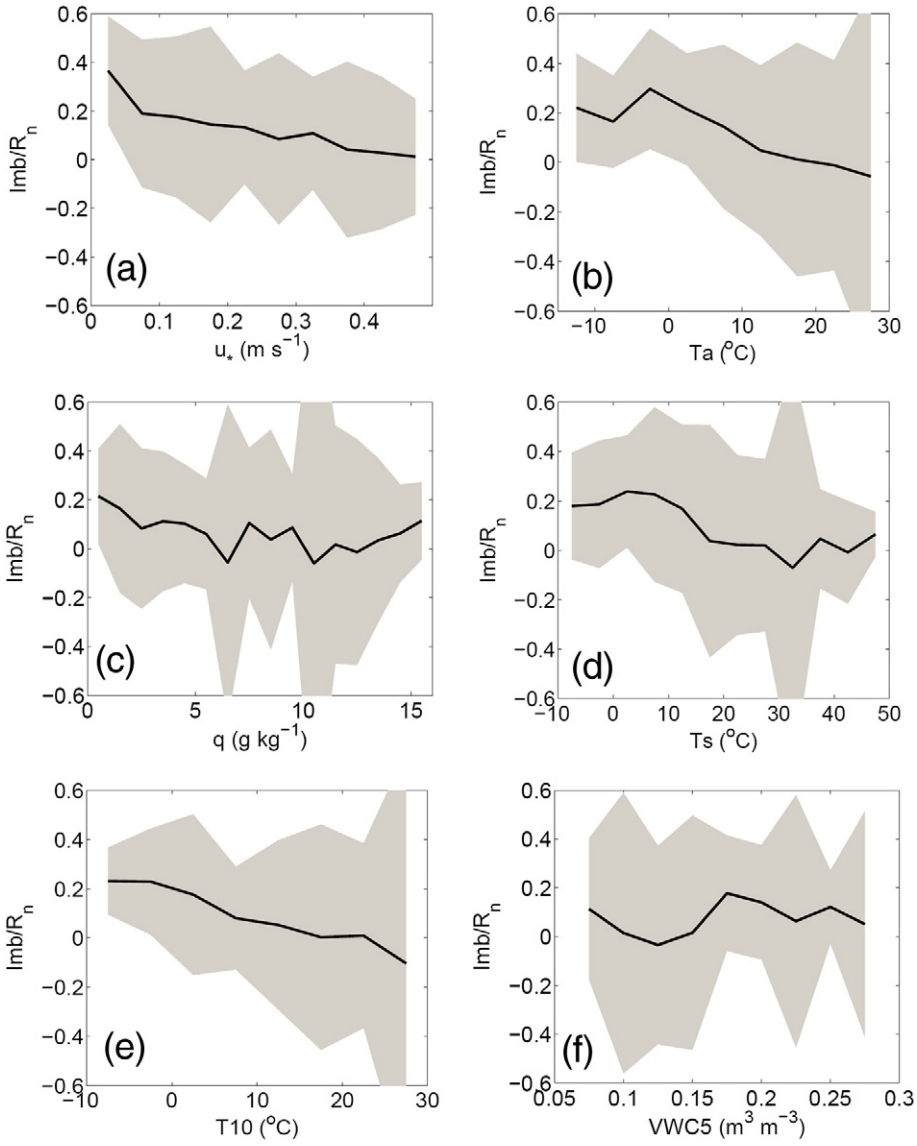

Fig. 12. Relationships between the ratio of energy imbalance and some air and soil variables during midday (modified after Fig. 5 in Cuxart et al., 2015), (a) Friction velocity, (b) air temperature, (c) specific humidity, (d) surface temperature, (e) soil temperature at 10cm depth, and (f) soil volumetric water content at 5cm depth.

investigated to evaluate the influence of human activities on regional climate in future studies.

Surface energy balance closures in our site were reasonably comparable to other sites, with the closure of 77.6% and 73.3% for the year of 2011 and 2012, respectively. However, the imbalance was large during midnight, related to the low turbulent intensity. The time delay of turbulent fluxes relative to the net radiation may cause large imbalance at 30-min timescale.

The semi-arid area of Loess Plateau is at the western edge of the East Asian summer monsoon-affected area and its climatic conditions, such as precipitation, have large interannual variations. Climate change could alter the water availability in the area, our study is limited to the analysis of only 2-years' variability of radiation and energy fluxes over the region. It is necessary to analyze long-term observation data or model results over this area to evaluate the influence of climate change on the energy partitioning.

Author contributions

Xing Chen and Ye Yu designed the study and are responsible for the integrity of the manuscript and wrote the manuscript. Xing Chen performed the analysis and all the calculations. Jinbei Chen contributed to data processing. Tangtang Zhang and Zhenchao Li contributed to data collecting. All authors discussed and commented on the manuscript.

Acknowledgements

This research was supported by the National Natural Science Foundation of China (Project No.41175009, No.41375001) and the National Key Basic Research Program of China (2014CB441404). Pingliang Land Surface Process & Severe Weather Research Station is a member of the Land Surface Process Observation Network, Chinese Academy of Sciences. We thank all the colleagues involved in the Loess Plateau Mesa Region Land Surface Process Field Experiment Series (LOPEXs) for their effort, sweat and contributions in setting up and maintaining instruments. We also thank the three anonymous reviewers for their valuable suggestions that greatly improved the manuscript.

Appendix A. Supplementary data

Supplementary data associated with this article can be found in the online version, at http://dx.doi.org/10.1016/j.atmosres.2016.03.003. These data include the Google map of the most important areas described in this article.

References

Baldocchi, D.D., 2008. Breathing of the terrestrial biosphere: lessons learned from a global network of carbon dioxide flux measurement systems. Aust. J. Bot. 56 (1), 1–26. http://dx.doi.org/10.1071/bt07151.

Baldocchi, D.D., Meyers, T., 1998. On using eco-physiological, micrometeorological and biogeochemical theory to evaluate carbon dioxide, water vapor and trace gas fluxes over vegetation: a perspective. Agric. For. Meteorol. 90 (1-2), 1–25. http://dx.doi.org/10.1016/s0168-1923(97)00072-5.

Baldocchi, D.D., Vogel, C.A., Hall, B., 1997. Seasonal variation of energy and water vapor exchange rates above and below a boreal jack pine forest canopy. J. Geophys. Res. D: Atmos. 102 (D24), 28939–28951. http://dx.doi.org/10.1029/96jd03325.

Baldocchi, D.D., Falge, E., Gu, L., Olson, R., Hollinger, D., Running, S., Anthoni, P., Bernhofer, C., Davis, K., Evans, R., Fuentes, J., Goldstein, A., Katul, G., Law, B., Lee, X., Malhi, Y., Meyers, T., Munger, W., Oechel, W., Paw, U.K.T., Pilegaard, K., Schmid, H.P., Valentini, R., Verma, S., Vesala, T., Wilson, K., Wofsy, S., 2001. FLUXNET: A new tool to study the temporal and spatial variability of ecosystem-scale carbon dioxide, water vapor, and energy flux densities. Bull. Am. Meteorol. Soc. 82 (11), 2415–2434. http://dx.doi.org/10.1175/1520-0477(2001)082<2415:fantts>2.3.co;2.

Barcza, Z., Kern, A., Haszpra, L., Kljun, N., 2009. Spatial representativeness of tall tower eddy covariance measurements using remote sensing and footprint analysis. Agric. For. Meteorol. 149 (5), 795–807. http://dx.doi.org/10.1016/j.agrformet.2008.10.021.

Betts, R.A., 2001. Biogeophysical impacts of land use on present-day climate: near-surface temperature change and radiative forcing. Atmos. Sci. Lett. 2 (1-4), 39–51. http://dx.doi.org/10.1006/asle.2001.0023.

Betts, A.K., Ball, J.H., Beljaars, A.C.M., Miller, M.J., Viterbo, P.A., 1996. The land surface-atmosphere interaction: a review based on observational and global modeling perspectives. J. Geophys. Res. 101 (D3), 7209. http://dx.doi.org/10.1029/95jd02135.

Bi, X., Gao, Z., Deng, X., Wu, D., Liang, J., Zhang, H., Sparrow, M., Du, J., Li, F., Tan, H., 2007. Seasonal and diurnal variations in moisture, heat, and CO_2 fluxes over grassland in the tropical monsoon region of southern China. J. Geophys. Res. 112 (D10). http://dx.doi.org/10.1029/2006jd007889.

Bruemmer, C., Falk, U., Papen, H., Szarzynski, J., Wassmann, R., Brueggemann, N., 2008. Diurnal, seasonal, and interannual variation in carbon dioxide and energy exchange in shrub savanna in Burkina Faso (West Africa). J. Geophys. Res. G: Biogeosci. 113 (G2). http://dx.doi.org/10.1029/2007jg000583.

Chen, S., Chen, J., Lin, G., Zhang, W., Miao, H., Wei, L., Huang, J., Han, X., 2009. Energy balance and partition in Inner Mongolia steppe ecosystems with different land use types. Agric. For. Meteorol. 149 (11), 1800–1809. http://dx.doi.org/10.1016/j.agrformet.2009.06.009.

Chen, X., Su, Z., Ma, Y., Sun, F., 2012. Analysis of land–atmosphere interactions over the north region of Mt. Qomolangma (Mt. Everest). Arct. Antarct. Alp. Res. 44 (4), 412–422. http://dx.doi.org/10.1657/1938-4246-44.4.412.

Chen, X., Yu, Y., Chen, J., Zhang, T., Li, Z., 2014. Study of estimation of soil heat flux at a wheat field in semi-arid area of Loess Plateau (in Chinese). Plateau Meteor. 33 (6), 1514–1525. http://dx.doi.org/10.7522/j.issn.1000-0534.2013.00091.

Cuxart, J., Conangla, L., Jimenez, M.A., 2015. Evaluation of the surface energy budget equation with experimental data and the ECMWF model in the Ebro Valley. J. Geophys. Res. 120 (3), 1008–1022. http://dx.doi.org/10.1002/2014jd022296.

Dickinson, R.E., Henderson-Sellers, A., Rosenzweig, C., Sellers, P.J., 1991. Evapotranspiration models with canopy resistance for use in climate models, a review. Agric. For. Meteorol. 54 (2-4), 373–388. http://dx.doi.org/10.1016/0168-1923(91)90014-h.

Eugster, W., Rouse, W.R., Pielke, R.A., McFadden, J.P., Baldocchi, D.D., Kittel, T.G.F., Chapin, F.S., Liston, G.E., Vidale, P.L., Vaganov, E., Chambers, S., 2000. Land–atmosphere energy exchange in Arctic tundra and boreal forest: available data and feedbacks to climate. Glob. Chang. Biol. 6, 84–115. http://dx.doi.org/10.1046/j.1365-2486.2000.06015.x.

Foken, T., 2008a. The energy balance closure problem: an overview. Ecol. Appl. 18 (6), 1351–1367. http://dx.doi.org/10.1890/06-0922.1.

Foken, T., 2008b. Micrometeorology. Springer-Verlag, Berlin Heidelberg.

Gao, Z., Lenschow, D.H., He, Z., Zhou, M., 2009. Seasonal and diurnal variations in moisture, heat and CO_2 fluxes over a typical steppe prairie in Inner Mongolia, China. Hydrol. Earth Syst. Sci. 13 (7), 987–998. http://dx.doi.org/10.5194/hess-13-987-2009.

Gockede, M., Rebmann, C., Foken, T., 2004. A combination of quality assessment tools for eddy covariance measurements with footprint modelling for the characterisation of complex sites. Agric. For. Meteorol. 127 (3-4), 175–188. http://dx.doi.org/10.1016/j.agrformet.2004.07.012.

Gu, L., Meyers, T., Pallardy, S.G., Hanson, P.J., Yang, B., Heuer, M., Hosman, K.P., Riggs, J.S., Sluss, D., Wullschleger, S.D., 2006. Direct and indirect effects of atmospheric conditions and soil moisture on surface energy partitioning revealed by a prolonged drought at a temperate forest site. J. Geophys. Res. 111 (D16). http://dx.doi.org/10.1029/2006jd007161.

Gu, L., Yao, J., Hu, Z., Zhao, L., 2015. Comparison of the surface energy budget between regions of seasonally frozen ground and permafrost on the Tibetan Plateau. Atmos. Res. 153 (0), 553–564. http://dx.doi.org/10.1016/j.atmosres.2014.10.012.

Guan, X., Huang, J., Guo, N., Bi, J., Wang, G., 2009. Variability of soil moisture and its relationship with surface albedo and soil thermal parameters over the Loess Plateau. Adv. Atmos. Sci. 26 (4), 692–700. http://dx.doi.org/10.1007/s00376-009-8198-0.

Hammerle, A., Haslwanter, A., Schmitt, M., Bahn, M., Tappeiner, U., Cernusca, A., Wohlfahrt, G., 2006. Eddy covariance measurements of carbon dioxide, latent and sensible energy fluxes above a meadow on a mountain slope. Bound.-Layer Meteorol. 122 (2), 397–416. http://dx.doi.org/10.1007/s10546-006-9109-x.

Holwerda, F., Bruijnzeel, L.A., Barradas, V.L., Cervantes, J., 2013. The water and energy exchange of a shaded coffee plantation in the lower montane cloud forest zone of central Veracruz, Mexico. Agric. For. Meteorol. 173, 1–13. http://dx.doi.org/10.1016/j.agrformet.2012.12.015.

Huang, J.P., Zhang, W., Zuo, J.Q., Bi, J.R., Shi, J.S., Wang, X., Chang, Z.L., Huang, Z.W., Yang, S., Zhang, B.D., Wang, G.Y., Feng, G.H., Yuan, J.Y., Zhang, L., Zuo, H.C., Wang, S.G., Fu, C.B., Chou, J.F., 2008. An overview of the semi-arid climate and environment research observatory over the Loess Plateau. Adv. Atmos. Sci. 25 (6), 906–921. http://dx.doi.org/10.1007/s00376-008-0906-7.

Kljun, N., Calanca, P., Rotach, M.W., Schmid, H.P., 2004. A simple parameterisation for flux footprint predictions. Bound.-Layer Meteorol. 112 (3), 503–523. http://dx.doi.org/10.1023/b:boun.0000030653.71031.96.

Lei, H., Yang, D., 2010. Interannual and seasonal variability in evapotranspiration and energy partitioning over an irrigated cropland in the North China Plain. Agric. For. Meteorol. 150 (4), 581–589. http://dx.doi.org/10.1016/j.agrformet.2010.01.022.

Leuning, R., van Gorsel, E., Massman, W.J., Isaac, P.R., 2012. Reflections on the surface energy imbalance problem. Agric. For. Meteorol. 156, 65–74. http://dx.doi.org/10.1016/j.agrformet.2011.12.002.

Li, Z.Q., Yu, G.R., Wen, X.F., Zhang, L.M., Ren, C.Y., Fu, Y.L., 2005. Energy balance closure at ChinaFLUX sites. Sci. China Ser. D 48, 51–62. http://dx.doi.org/10.1360/05zd0005.

Li, H., Zhang, Q., Shi, J., Zhao, J., Wang, S., 2012a. A study of the parameterization of land-surface processes over the natural vegetation surface of Loess Plateau. Acta Meteorol. Sin. 70 (5), 1137–1148 (doi:0577-6619(2012)70:5<1137:htgyzr>2.0.tx;2-9).

Li, H., Zhang, Q., Wang, C., Yang, F., Zhao, J., 2012b. The influences of air heat storage, plant photosynthesis and soil water movement on surface energy balance over the loess plateau (in Chinese). Acta Phys. Sin. 61 (15). http://dx.doi.org/10.7498/aps.61.159201.

Liu, H., Feng, J., 2012. Seasonal and interannual variations of evapotranspiration and energy exchange over different land surfaces in a semiarid area of China. J. Appl. Meteorol. Climatol. 51 (10), 1875–1888. http://dx.doi.org/10.1175/jamc-d-11-0229.1.

Liu, H., Dong, W., Fu, C., Shi, L., 2004. The long-term field experiment on aridification and the ordered human activity in semi-arid area at Tongyu, Northeast China (in

Chinese). Clim. Environ. Res. 9 (2), 378–389 (doi:1006-9585(2004)9:2<378:bghdqj-2.0.tx;2-y).
Liu, H., Tu, G., Dong, W., 2008a. Variation of surface albedo over different land surfaces in semiarid area of China (in Chinese). Chin. Sci. Bull. 53 (10), 1220–1227 (doi:0023-074x(2008)53:10<1220:bghqbt>2.0.tx;2-3).
Liu, H., Tu, G., Fu, C., Shi, L., 2008b. Three-year variations of water, energy and CO_2 fluxes of cropland and degraded grassland surfaces in a semi-arid area of Northeastern China. Adv. Atmos. Sci. 25 (6), 1009–1020. http://dx.doi.org/10.1007/s00376-008-1009-1.
Ma, Y.M., Su, Z.B., Koike, T., Yao, T.D., Ishikawa, H., Ueno, K., Menenti, M., 2003. On measuring and remote sensing surface energy partitioning over the Tibetan Plateau — from GAME/Tibet to CAMP/Tibet. Phys. Chem. Earth 28 (1-3), 63–74. http://dx.doi.org/10.1016/s1474-7065(03)00008-1.
Mauder, M., Cuntz, M., Druee, C., Graf, A., Rebmann, C., Schmid, H.P., Schmidt, M., Steinbrecher, R., 2013. A strategy for quality and uncertainty assessment of long-term eddy-covariance measurements. Agric. For. Meteorol. 169, 122–135. http://dx.doi.org/10.1016/j.agrformet.2012.09.006.
Meyers, T.P., Hollinger, S.E., 2004. An assessment of storage terms in the surface energy balance of maize and soybean. Agric. For. Meteorol. 125 (1-2), 105–115. http://dx.doi.org/10.1016/j.agrformet.2004.03.001.
Miao, H., Chen, S., Chen, J., Zhang, W., Zhang, P., Wei, L., Han, X., Lin, G., 2009. Cultivation and grazing altered evapotranspiration and dynamics in Inner Mongolia steppes. Agric. For. Meteorol. 149 (11), 1810–1819. http://dx.doi.org/10.1016/j.agrformet.2009.06.011.
Peters, E.B., Hiller, R.V., McFadden, J.P., 2011. Seasonal contributions of vegetation types to suburban evapotranspiration. J. Geophys. Res. 116. http://dx.doi.org/10.1029/2010jg001463.
Pielke, R.A., Avissar, R., Raupach, M., Dolman, A.J., Zeng, X.B., Denning, A.S., 1998. Interactions between the atmosphere and terrestrial ecosystems: influence on weather and climate. Glob. Chang. Biol. 4 (5), 461–475. http://dx.doi.org/10.1046/j.1365-2486.1998.t01-1-00176.x.
Ryu, Y., Baldocchi, D.D., Ma, S., Hehn, T., 2008. Interannual variability of evapotranspiration and energy exchange over an annual grassland in California. J. Geophys. Res. 113 (D9). http://dx.doi.org/10.1029/2007jd009263.
Su, Z., 2002. The Surface Energy Balance System (SEBS) for estimation of turbulent heat fluxes. Hydrol. Earth Syst. Sci. 6 (1), 85–99. http://dx.doi.org/10.5194/hess-6-85-2002.
Su, Z., Zhang, T., Ma, Y., Jia, L., Wen, J., 2006. Energy and water cycle over the Tibetan Plateau: surface energy balance and turbulent heat fluxes (in Chinese). Adv. Earth Sci. 21 (12), 1224–1236 (doi:1001-8166(2006)21:12<1224:eawcot>2.0.tx;2-c).
Suyker, A.E., Verma, S.B., 2008. Interannual water vapor and energy exchange in an irrigated maize-based agroecosystem. Agric. For. Meteorol. 148 (3), 417–427. http://dx.doi.org/10.1016/j.agrformet.2007.10.005.
Wang, G., Huang, J., Guo, W., Zuo, J., Wang, J., Bi, J., Huang, Z., Shi, J., 2010. Observation analysis of land–atmosphere interactions over the Loess Plateau of northwest China. J. Geophys. Res. 115. http://dx.doi.org/10.1029/2009jd013372.
Wang, S., Zhang, Q., Wang, X., Li, H., Zhang, Z., 2013. Comparison of the water and heat characteristics of bare soil in different climate region of the Loess Plateau (in Chinese). J. Desert Res. 33 (4), 1166–1173 (doi:1000-694x(2013)33:4<1166:htgybt-2.0.tx;2-#).
Wen, J., Wei, Z., Lü, S., Chen, S., Ao, Y., Liang, L., 2007. Autumn daily characteristics of land surface heat and water exchange over the Loess Plateau mesa in China. Adv. Atmos. Sci. 24 (2), 301–310. http://dx.doi.org/10.1007/s00376-007-0301-9.
Wen, J., Wang, L., Wei, Z.G., 2009. An overview of the LOess Plateau mesa region land surface process field EXperiment series (LOPEXs). Hydrol. Earth Syst. Sci. 13 (6), 945–951. http://dx.doi.org/10.5194/hess-13-945-2009.
Wilson, K.B., Baldocchi, D.D., 2000. Seasonal and interannual variability of energy fluxes over a broadleaved temperate deciduous forest in North America. Agric. For. Meteorol. 100 (1), 1–18. http://dx.doi.org/10.1016/s0168-1923(99)00088-x.
Wilson, K.B., Baldocchi, D.D., Aubinet, M., Berbigier, P., Bernhofer, C., Dolman, H., Falge, E., Field, C., Goldstein, A., Granier, A., Grelle, A., Halldor, T., Hollinger, D., Katul, G., Law, B.E., Lindroth, A., Meyers, T., Moncrieff, J., Monson, R., Oechel, W., Tenhunen, J., Valentini, R., Verma, S., Vesala, T., Wofsy, S., 2002. Energy partitioning between latent and sensible heat flux during the warm season at FLUXNET sites. Water Resour. Res. 38 (12), 1294. http://dx.doi.org/10.1029/2001wr000989.
Wu, J., Guan, D., Han, S., Shi, T., Jin, C., Pei, T., Yu, G., 2007. Energy budget above a temperate mixed forest in northeastern China. Hydrol. Process. 21 (18), 2425–2434. http://dx.doi.org/10.1002/hyp.6395.
Yao, J., Zhao, L., Gu, L., Qiao, Y., Jiao, K., 2011. The surface energy budget in the permafrost region of the Tibetan Plateau. Atmos. Res. 102 (4), 394–407. http://dx.doi.org/10.1016/j.atmosres.2011.09.001.
Yu, G., Wen, X., Sun, X., Tanner, B.D., Lee, X., Chen, J., 2006. Overview of ChinaFLUX and evaluation of its eddy covariance measurement. Agric. For. Meteorol. 137 (3-4), 125–137. http://dx.doi.org/10.1016/j.agrformet.2006.02.011.
Yue, P., Li, Y., Zhang, Q., Zhang, L., 2012. Surface energy-balance closure in a gully region of the Loess Plateau at SACOL on eastern edge of Tibetan Plateau. J. Meteorol. Soc. Jpn. 90C, 173–184. http://dx.doi.org/10.2151/jmsj.2012-C12.
Zhang, T., Wen, J., Su, Z., van der Velde, R., Timmermans, J., Liu, R., Liu, Y., Li, Z., 2009. Soil moisture mapping over the Chinese Loess Plateau using ENVISAT/ASAR data. Adv. Space Res. 43 (7), 1111–1117. http://dx.doi.org/10.1016/j.asr.2008.10.030.
Zhang, Q., Sun, Z., Wang, S., 2011a. Analysis of variation regularity of land-surface physical quantities over the Dingxi region of the Loess Plateau. Chin. J. Geophys. 54 (4), 436–447. http://dx.doi.org/10.1002/cjg2.1627.
Zhang, Q., Wang, S., Wen, X., Li, H., 2011b. Experimental study of the imbalance of water budget over the Loess Plateau of China. Acta Meteorol. Sin. 25 (6), 765–773. http://dx.doi.org/10.1007/s13351-011-0607-5.
Zhang, Q., Huang, J., Zhang, L., Zhang, L., 2013a. Warming and drying climate over Loess plateau area in China and its effect on land surface energy exchange (in Chinese). Acta Phys. Sin. 62 (13). http://dx.doi.org/10.7498/aps.62.139202.
Zhang, Q., Li, H., Zhang, L., Yue, P., Shi, J., 2013b. Responses of the land-surface process and its parameters over the natural vegetation underlying surface of the middle of Gansu in loess plateau to precipitation fluctuation (in Chinese). Acta Phys. Sin. 62 (1). http://dx.doi.org/10.7498/aps.62.019201.
Zhang, T., Wen, J., Wei, Z., van der Velde, R., Li, Z., Liu, R., Lv, S., Chen, H., 2014. Land–atmospheric water and energy cycle of winter wheat, Loess Plateau, China. Int. J. Clim. http://dx.doi.org/10.1002/joc.3891.
Zuo, J., Huang, J., Wang, J., Zhang, W., Bi, J., Wang, G., Li, W., Fu, P., 2009. Surface turbulent flux measurements over the Loess Plateau for a semi-arid climate change study. Adv. Atmos. Sci. 26 (4), 679–691. http://dx.doi.org/10.1007/s00376-009-8188-2.